

Sugar-Alcohol Complexes of Palladium(II): On the Variable Rigidity of Open-Chain Carbohydrate Ligands**

Thorsten Allscher, Xaver Kästele, Gerhard Kettenbach, Peter Klüfers,* and Thomas Kunte^[a]

Abstract: The C₄, C₅, and C₆ sugar alcohols erythritol (Eryt), D-threitol (D-Thre), D-arabitol (D-Arab), ribitol (Ribt), xylitol (Xylt), dulcitol (Dulc), and D-mannitol (D-Mann) form chelate complexes upon dissolution in Pd-en, an aqueous solution of [Pd^{II}(en)(OH)₂]. Stability rules are derived from the proportion of a respective species in the solution equilibrium. Crystal-structure analysis supports the NMR spectroscopic results for a series of binuclear compounds that contain the sugar alcohols as tetraanionic polyolato ligands: [Pd₂(en)₂(ErytH₋₄)]·10H₂O, [Pd₂(en)₂(D-Arab1,2;3,4H₋₄)]·7H₂O, [Pd₂(en)₂(Xylt1,2;3,4H₋₄)]·4H₂O,

[Pd₂(en)₂(D-Mann1,2;3,4H₋₄)]·5H₂O, and [Pd₂(en)₂(Dulc2,3;4,5H₋₄)]·6H₂O. In the case of the pentitols and hexitols, the metalated tetraanions are stabilized by intramolecular hydrogen bonds. The hydrogen bonds uniformly connect an alkoxide acceptor to the hydroxy donor group located at the δ carbon atom. As a consequence of hydrogen bonding, the open-chain carbohydrate ligands become rigid. Crystal-structure analysis provides information

on the configurational requirements for rigidity. According to these rules, the hydrogen-bond-supported Dulc2,3;4,5H₋₄ tetraanion provides a geometrically persistent ligating pattern. Intramolecular hydrogen bonding seems to be the most-competitive variable to metalation of a polyol. [Pd₂(tm-2,1:3,2-tet)(OH)₃]OH (tm-2,1:3,2-tet = 1,3-bis(2'-dimethylaminoethyl)hexahydro-pyrimidine) is a metallizing agent that can force full metalation even in a case as intractable as that of dulcitol. Accordingly, [Pd₄(tm-2,1:3,2-tet)₂(DulcH₋₆)]Cl₂·16H₂O contains the fully deprotonated hexitol as the ligand.

Keywords: alcohols · alditols · carbohydrates · diolato ligands · palladium

Introduction

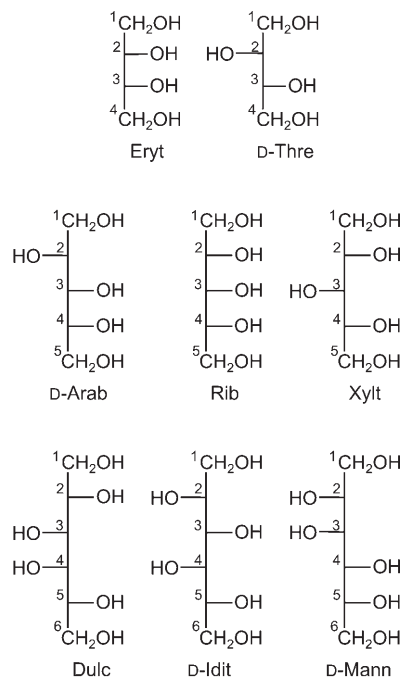
Aqueous [Pd(en)(OH)₂] (Pd-en) and solutions of related palladium(II) complexes with an N₂ set of ligating atoms are currently the most-versatile reagents for the reliable transformation of the diol groups of a carbohydrate into dianionic ligands in chelation to the PdN₂ moiety. The stability of the complexes is underlined by the fact that complete metalation can be achieved. Hence, all the vicinal diol groups of an anomeric mixture of α- and β-D-glucopyranose were transformed into palladacycles when glucose formed [Pd(en)]₂(α-D-Glcp1,2;3,4H₋₄) and [Pd(en)]₂(β-D-

Glcp1,2;3,4H₋₄) upon reaction with Pd-en (Glc = glucopyranose).^[1,2] The same holds true for glucosides such as cellulose, whose O2/3 diol groups were entirely metalated in the course of cellulose dissolution in Pd-en.^[3] In view of these results, the reaction of open-chain carbohydrate derivatives is intriguing. Entire, or in this case, threefold metalation of a hexitol such as dulcitol appeared inaccessible in preliminary experiments with Pd-en. This result was particularly annoying when the significance of open-chain derivatives in carbohydrate chemistry is considered. There exist not only stable open-chain compounds such as sugar alcohols and aldonic and aldaric acids, but also, most challengingly, the unstable open-chain forms of the monosaccharides themselves. The development of spectator-ligand-metal fragments that can be used as tools to stabilize and manipulate the most-reactive forms of a monosaccharide, that is, the aldehyde and aldehyde hydrate, is therefore a major goal of carbohydrate-directed coordination chemistry. The aim of this work is thus to clarify the reasons for restricted metal bonding to open-chain polyol ligands and to develop a strategy to overcome these restrictions. For this purpose, the typical ligand

[a] T. Allscher, X. Kästele, Dr. G. Kettenbach, Prof. Dr. P. Klüfers, Dr. T. Kunte
Department of Chemistry and Biochemistry
Ludwig Maximilian University
Butenandtstraße 5–13, 81377 Munich (Germany)
Fax: (+49) 89-2180-77407
E-mail: kluef@cup.uni-muenchen.de

[**] Polyol Metal Complexes, Part 57. For Part 56, see: T. Allscher, P. Klüfers, O. Labisch, *Carbohydr. Res.* **2007**, DOI: 10.1016/j.corres.2007.04.025.

properties of representative sugar alcohols (Scheme 1) with up to six hydroxy groups were investigated, and the most-stable ligating forms were identified. Finally, the spectator ligand was adapted to support a metalation pattern so stable that even the most-conservative ligating moiety, the tetradentate Dulc_{2,3;4,5H₄} tetraanion, was broken up.



Scheme 1. Fischer projections, including atomic numbering, of the sugar alcohols used in this work.

Results and Discussion

Ethanediol, Propane-1,3-diol, and Glycerol: Five- versus Six-Membered Ring Chelation

To provide basic spectroscopic and structural data, the investigation began with some simple hydroxy compounds. ¹³C and ¹H NMR spectra of equimolar amounts of ethanediol dissolved in 0.2 M Pd-en revealed complex formation even for this, the least-acidic 1,2-diol in this work. Under the conditions chosen, about 70% of the diol formed the diolato complex with the Pd(en) moiety. Reaction of double the molar amount of palladium reagent with ethylene glycol at a Pd concentration of 0.32 M left about 10% of the diol uncomplexed.

The triol glycerol was found as a bidentate triolato(2-) ligand bonded to palladium. At a Pd/glycerol molar ratio of 2:1, only a small amount of free triol was detected in the ¹³C NMR spectrum. The bonding mode of the triol is almost exclusively that of a κ²O¹,O² five-ring chelator with minute amounts of the κ²O¹,O³ six-ring isomer detectable in the NMR spectra. To confirm the assignment of the NMR signals, propane-1,3-diol was also investigated. As expected, propane-1,3-diolate turned out to be a much poorer ligand than the 1,2-diol moiety due to the lower acidity of the

former. In 0.2 M Pd-en, less than 20% of the diol was observed to be bonded to palladium. However, complex formation was significant enough to show the characteristic spectral features of the different bonding modes. Table 1

Table 1. ¹³C NMR chemical shifts (ppm) of Pd-ethanediol, -propane-1,3-diol, and -glycerol complexes.^[a]

	C1	C2	C3
[Pd(en)(EthdH ₂)]	72.9		
(Δδ)	(8.5)		
[Pd(en)(PrndH ₂)]	63.9	40.0	
(Δδ)	(3.5)	(4.4)	
[Pd(en)(Glyc1,2H ₂)]	73.1	81.5	63.5
(Δδ)	(9.9)	(8.8)	(0.4)
[Pd(en)(Glyc1,3H ₂)]	67.4	74.0	
(Δδ)	(4.3)	(1.3)	

[a] Atoms are numbered as in Scheme 1. The signals of the en ligands are omitted. Δδ is the difference between the chemical shifts of the free and the palladium-binding polyols taken from the same spectrum in each case. Δδ values that indicate a CIS due to 1,2-diolate coordination are in bold. The Glyc1,3 species (last entry) is present as a trace component. Ethd = ethane-1,2-diol, Glyc = glycerol, Prnd = propane-1,3-diol.

shows the typical coordination-induced shift (CIS; Δδ) values, which are of diagnostic value in the case of the 1,2-diolato bonding mode. For this mode, the ¹³C NMR signals of the carbon atoms that bear a palladium-bonded oxygen atom were shifted downfield by about 10 ppm. As was pointed out for levoglucosane as another example of a 1,3-diol,^[3b] the CIS values for this bonding mode are less informative. Attempts to crystallize any of these forms were successful for the propanediolato complex only. The crystal-structure analysis revealed the expected bonding pattern.^[4] Crystals of the ethanediol and glycerol complexes were obtained in low quality only. A preliminary structure analysis of the glycerol derivative confirmed the spectroscopic assignment of a five-membered chelate ring.

Erythritol and Threitol: The Basic Binucleating Bis(diolato) Patterns

In terms of the ¹³C NMR spectra, the isomeric tetraols erythritol (Eryt) and D-threitol (D-Thre) form the fully metalated [Pd₂(en)₂(tetraol1,2;3,4H₄)] species in aqueous solutions of Pd/tetraol of molar ratio 3:1 (3:1 solutions). With erythritol, the binuclear species is the main species in solution, whereas, as a rough estimate, only half of the D-threitol binds two Pd(en) moieties; the other half acts as a ligand in the mononuclear [Pd(en)(D-Thre2,3H₂)] species. The minor tetraolato species (less than about 10% of tetraol-containing complexes) are [Pd(en)(D-Thre1,2H₂)], [Pd(en)(Eryt-1,2H₂)], and, even less abundant, [Pd(en)(Eryt2,3H₂)] (Table 2). No signals of free tetraol were observed at the 3:1 molar ratio. The pronounced stability of binuclear [Pd₂(en)₂(Eryt1,2;3,4H₄)] and mononuclear [Pd(en)(D-Thre2,3H₂)] in the respective solutions dominates the species distribution in 1:1 solutions as well. In the case of erythritol, about one quarter of the tetraol was found as a ligand

Table 2. ^{13}C NMR chemical shifts (ppm) of the observed solution species in solutions of tetritol of different Pd-en/tetritol molar ratios.^[a]

	C1	C2	C3	C4	3:1	1:1
D-Thre	63.3	72.3			n.d.	–
[Pd(en)(D-Thre1,2H ₂)]	72.2	81.9	73.5	63.7	–	+
($\Delta\delta$)	(8.9)	(9.6)	(1.2)	(0.4)		
[Pd(en)(D-Thre2,3H ₂)]	64.8	82.0			++	+++
($\Delta\delta$)	(1.5)	(9.7)				
[Pd ₂ (en) ₂ (D-Thre1,2;3,4H ₄)]	72.6	84.1			++	–
($\Delta\delta$)	(9.3)	(11.8)				
Eryt	63.3	72.7			n.d.	+
[Pd(en)(Eryt1,2H ₂)]	73.7	82.0	73.7	64.3	–	++
($\Delta\delta$)	(10.4)	(9.3)	(1.0)	(1.0)		
[Pd(en)(Eryt2,3H ₂)]	62.5	82.1			trace	–
($\Delta\delta$)	(–0.8)	(9.4)				
[Pd ₂ (en) ₂ (Eryt1,2;3,4H ₄)]	75.4	83.8			++++	+
($\Delta\delta$)	(12.1)	(11.1)				

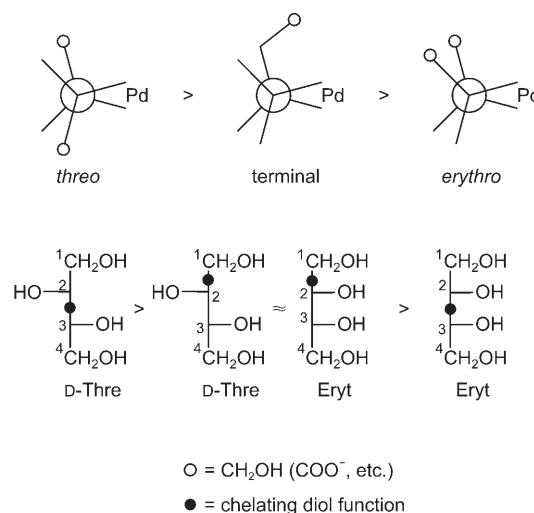
[a] Atoms are numbered as in Scheme 1. The signals of the en ligands are omitted. $\Delta\delta$ values that indicate a CIS due to 1,2-diolate coordination are in bold. As a rough assessment of the molar concentrations of individual species, “+” = about $\frac{1}{4}$ of the total tetritol concentration, “–” = about 10% or less, “trace” = an NMR-detectable species, “n.d.” = not detected.

in the binuclear complex despite the fact that an equivalent amount of erythritol remains uncomplexed in the equimolar solutions. With D-threitol, the [Pd(en)(D-Thre2,3H₂)] complex is almost the only species in 1:1 solutions. Hence, threitol is the “normal case”, as the most-acidic hydroxy groups are deprotonated to form a complex of the expected molar ratio (compare the results of Andrews et al. for mononuclear bis(phosphane)tetraolato(2–)platinum(II) complexes^[5]).

As a result, the binding of a single metal atom to the diol group of a tetraol follows the stability relationship *threo* > *terminal* > *erythro*. This result agrees with stereochemical considerations: the *threo* configuration of a central diol moiety allows the bulky substituents (hydroxymethyl in the case of a tetraol) to be far apart, whereas in an *erythro*-configured diol, a conformation closer to an eclipsed arrangement of the substituents is forced. Terminal metalation of a tetraol appears more favorable than *erythro* coordination as a result of the combination of low steric strain on the one hand and deprotonation of a less-acidic terminal hydroxy group on the other. The rule is illustrated in Scheme 2 by means of Fischer and Newman projections.

Attempts to crystallize some of the tetraol–palladium complexes were successful for the binuclear erythritolato compound, which was obtained in the form of yellow crystals from palladium-rich solutions. Crystals of [Pd₂(en)₂(Eryt1,2;3,4H₄)]·10H₂O (**1**), the decahydrate of the main solution species, are composed of almost-flat, centrosymmetric molecules (Figure 1 and Table 3) whose structure resembles that of the ammine analogue.^[6] The alkoxo O atoms of the fully deprotonated, tetraanionic erythritolato ligands act as hydrogen-bond acceptors in two H bonds each.

The most-stable Pd₁–Eryt species, [Pd(en)(Eryt1,2H₂)], is clearly stabilized by an intramolecular hydrogen bond from the O4–H donor to the O2 acceptor. Though not sub-



Scheme 2. Complex stability for various tetraol binding modes (see text).

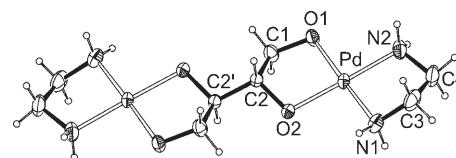


Figure 1. ORTEP plot (ellipsoids drawn at 60% probability) of the C₁-symmetric erythritol complex in **1**. Bond lengths (Å): Pd–O1 2.002(2), Pd–O2 2.008(2), Pd–N2 2.032(3), Pd–N1 2.040(2), O1–C1 1.423(4), O2–C2 1.433(3), C1–C2 1.513(4), C2–C2' 1.516(5). Bond and torsion angles (°): O1–Pd–O2 85.37(8), N2–Pd–N1 83.67(11), C1–C2–C2' 112.8(3); O1–C1–C2–O2 52.0(3), N1–C3–C4–N2 –53.2(3).

stantiated by crystal-structure data on a palladium compound, structure analysis of a salt of the related [Co^{III}-(tren)(Eryt1,2H₂)]⁺ ion (tren = *N,N,N*-triaminoethylamine) showed the O4–H···O2 bond.^[7] In the case of threitol, the O3 hydroxy group would be in an unfavorable position in the O4–H···O2 hydrogen-bonded conformation. Hence, the analogous complex with a D-Thre1,2H₂ ligand is only a minor species in solution.

D-Arabitol, Ribitol, and Xylitol: Hydrogen-Bond-Supported *erythro* and *threo* Patterns

The pentitols D-arabitol (D-Arab), ribitol (Ribt), and xylitol (Xylt) exhibit rather different bonding capabilities. Whereas ribitol and xylitol are, under full metalation conditions, restricted to an *erythro*- and *threo*-configured bis(diolato) pattern, respectively, D-arabitol is expected to bind both as a *D-threo* (C1–C4) or *erythro* (C2–C5) bisdiol ligand.

However, despite this presumed ambiguity of the latter pentitol, the ^{13}C NMR spectra of D-arabitol in excess Pd-en showed five polyol signals of a dominant component, which were assigned to the *erythro*-linked bis(diolato) binding mode (Table 4). The structure of the Pd₂–D-Arab species was unravelled by crystal-structure analysis. The binuclear-complex molecules in yellow crystals of [Pd₂(en)₂(D-Arab-2,3;4,5H₄)]·7H₂O (**2**; Table 3), which were isolated from 3:1

Table 3. Crystallographic data of 1–4.

	1	2	3	4
Net formula	C ₈ H ₄₂ N ₄ O ₁₄ Pd ₂	C ₈ H ₃₈ N ₄ O ₁₂ Pd ₂	C ₉ H ₃₂ N ₄ O ₉ Pd ₂	C ₁₀ H ₃₆ N ₄ O ₁₁ Pd ₂
<i>M_r</i> [g mol ⁻¹]	631.26	607.26	553.21	601.25
Crystal size [mm]	0.25 × 0.20 × 0.13	0.33 × 0.13 × 0.10	0.23 × 0.11 × 0.02	0.40 × 0.25 × 0.04
<i>T</i> [K]	298(3)	200(3)	200(3)	200(3)
Diffractometer	Stoe IPDS	Stoe IPDS	Stoe IPDS	Stoe IPDS
Crystal system	triclinic	triclinic	monoclinic	monoclinic
Space group	<i>P</i> $\bar{1}$	<i>P</i> 1	<i>C</i> 2/ <i>c</i>	<i>P</i> 2 ₁
<i>a</i> [Å]	7.334(2)	7.451(2)	26.436(2)	8.7495(9)
<i>b</i> [Å]	9.048(2)	9.259(2)	7.5466(7)	14.1545(9)
<i>c</i> [Å]	9.989(2)	9.463(2)	18.895(1)	9.0350(8)
α [°]	82.81(2)	114.31(2)	90	90
β [°]	78.38(2)	89.58(2)	91.066(7)	110.41(1)
γ [°]	68.89(2)	106.11(2)	90	90
<i>V</i> [Å ³]	604.7(2)	567.3(2)	3769.0(5)	1048.7(2)
<i>Z</i>	1	1	8	2
ρ_{calc} [g cm ⁻³]	1.7335(6)	1.7775(5)	1.9499(3)	1.9041(3)
μ [mm ⁻¹]	1.550	1.642	1.956	1.772
Absorption correction	numerical	numerical	numerical	numerical
Transmission factors	0.8507–0.9112	0.7102–0.8689	0.7585–0.9614	0.6223–0.9427
Reflections measured	7607	5935	7632	10070
<i>R</i> _{int}	0.0259	0.0191	0.0488	0.0202
Mean $\sigma(I)/I$	0.0218	0.0191	0.0689	0.0245
θ range	3.02–28.00	2.63–28.07	2.16–25.73	2.41–27.88
Observed refls.	2359	4426	2581	4224
<i>x</i> , <i>y</i> (weighting scheme)	0.0282, 0.1168	0.0369, 0.2361	0.0289, 0	0.0195, 0
Flack parameter		0.04(3)		–0.02(2)
Reflections in refinement	2606	4699	3516	4684
Parameters	204	360	246	388
Restraints	14	7	0	1
<i>R</i> (<i>F</i> _{obs})	0.0189	0.0205	0.0314	0.0164
<i>R</i> _w (<i>F</i> ²)	0.0439	0.0585	0.0631	0.0346
<i>S</i>	1.051	1.125	0.872	0.962
Shift/error _{max}	–0.002	0.002	0.001	0.007
Max. electron density [e Å ⁻³]	0.582	0.567	1.043	0.410
Min. electron density [e Å ⁻³]	–0.635	–0.740	–0.677	–0.309

solutions, are closely related to the complex molecules in 1. Upon examination of their structure in Figure 2, one's attention is drawn to an additional feature of the arabitol complex. A short, intramolecular O1–H...O4 hydrogen bond, which uses the free hydroxy group as the donor, is present. In relation to the carbon atom (α position) bound to the acceptor oxygen atom, the carbon atom of the donor hydroxy group is in the δ position, and this bond is thus referred to as a δ hydrogen bond. Compared with erythritol, the δ bond stabilizes the binuclear species to such an extent that the monometalated species was observed in the 3:1 solutions in trace amounts only.

An analogous intramolecular hydrogen bond appears to be the reason for a relatively high content of binuclear species derived from the *threo*-linked bis-(diolato) moiety in xylitol. Contrary to the spectroscopic result obtained for the parent bisdiol threitol, the Pd₂ com-

Table 4. ¹³C NMR chemical shifts (ppm) of the observed solution species in pentitol solutions of different Pd-en/pentitol molar ratios.^[a]

	C1	C2	C3	C4	C5	3:1	2:1	1:1
D-Arab	63.7	70.9	71.1	71.6	63.6	n.d.	n.d.	+
[Pd(en)(D-Arab2,3H ₋₂)]	65.3	81.4	82.6	73.2	64.5	trace	–	++
($\Delta\delta$)	(1.6)	(10.5)	(11.5)	(1.6)	(0.9)			
[Pd ₂ (en) ₂ (D-Arab2,3;4,5H ₋₄)]	64.0	85.8	86.3	83.5	73.4	++++	++++	+
($\Delta\delta$)	(0.3)	(14.9)	(15.2)	(11.9)	(9.8)			
Ribt	63.0	72.7	72.9			n.d.	n.d.	–
[Pd(en)(Ribt1,2H ₋₂)]	72.6	82.4	74.5	72.3	62.8	trace	–	++
($\Delta\delta$)	(9.6)	(9.7)	(1.6)	(–0.4)	(–0.2)			
[Pd(en)(Ribt2,3H ₋₂)]	64.5	81.8	82.6	72.2	63.1	trace	–	++
($\Delta\delta$)	(1.5)	(9.1)	(9.7)	(–0.5)	(0.1)			
[Pd ₂ (en) ₂ (Ribt1,2;3,4H ₋₄)]	74.9	82.4	84.2	81.9	63.2	+++	+++	–
($\Delta\delta$)	(11.9)	(9.7)	(11.3)	(9.2)	(0.2)			
[Pd ₂ (en) ₂ (Ribt1,2;4,5H ₋₂)]	72.2	82.2	74.7			+	+	trace
($\Delta\delta$)	(9.2)	(9.5)	(1.8)					
Xylt	63.3	72.6	71.4			n.d.	n.d.	–
[Pd(en)(Xylt2,3H ₋₂)]	65.2	80.5	81.0	73.8	63.1	–	+	+++
($\Delta\delta$)	(1.9)	(7.9)	(9.6)	(1.2)	(–0.2)			
[Pd(en)(Xylt1,2H ₋₂)]	71.9	81.3	72.4	71.7	63.8	trace	–	–
($\Delta\delta$)	(8.6)	(8.7)	(1.0)	(–0.9)	(0.5)			
[Pd ₂ (en) ₂ (Xylt1,2;3,4H ₋₄)]	71.4	84.1	86.4	80.4	64.7	+++	++	–
($\Delta\delta$)	(8.1)	(11.5)	(15.0)	(7.8)	(1.4)			
[Pd ₂ (en) ₂ (Xylt1,2;4,5H ₋₂)]	73.2	81.6	71.7			–	–	trace
($\Delta\delta$)	(9.9)	(9.0)	(0.3)					

[a] Atoms are numbered as in Scheme 1. The signals of the en ligands are omitted. $\Delta\delta$ values that indicate a CIS due to 1,2-diolate coordination are in bold. As a rough assessment of the molar concentrations of individual species, “+” = about 1/4 of the total pentitol concentration, “–” = about 10% or less, “trace” = NMR-detectable species, “n.d.” = not detected.

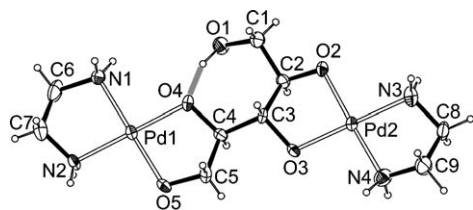


Figure 2. ORTEP plot (ellipsoids drawn at 60% probability) of the arabitol complex in **2**. Bond lengths (Å): Pd1–O4 2.001(5), Pd1–O5 1.991(6), Pd1–N1 2.055(6), Pd1–N2 2.034(6), Pd2–O2 2.010(5), Pd2–O3 2.013(4), Pd2–N3 2.047(6), Pd2–N4 2.033(7), C1–O1 1.434(4), C2–O2 1.421(9), C3–O3 1.441(9), C4–O4 1.427(9), C5–O5 1.438(9), C1–C2 1.531(7), C2–C3 1.532(10), C3–C4 1.534(3), C4–C5 1.513(10). Bond and torsion angles (°): O4–Pd1–O5 84.8(2), N1–Pd1–N2 84.3(3), O2–Pd2–O3 84.2(2), N3–Pd2–N4 83.1(3), C2–C3–C4 115.3(5), C1–C2–C3 116.7(5), C3–C4–C5 113.9(4), C2–C3–O3 105.5(5), C1–C2–O2 106.4(5), C2–C1–O1 112.5(4); O2–C2–C3–O3 58.4(8), O4–C4–C5–O5 50.1(8). Donor–acceptor distance in the intramolecular hydrogen bond: O1...O4 2.511 Å.

plex was found as the main solution species at a Pd/xylitol molar ratio of 3:1, although the Pd₂ species is not as predominant as with arabitol. Accordingly, the expected mononuclear species [Pd(en)(Xylt2,3H₂)], which is the racemic (due to equivalence with [Pd(en)(Xylt3,4H₂)] hydroxymethyl homologue of the predominant [Pd(en)(D-Thre2,3H₂)] parent complex, is a clearly detectable minor species in the case of xylitol in excess Pd-en (Table 4). The structure of the binuclear xylitol complex was determined by X-ray crystallography. Yellow crystals of [Pd₂(en)₂(Xylt1,2;3,4H₄)]·4H₂O (**3**; Table 3) with a relatively low water content are composed of the complex molecules depicted in Figure 3. In fact, the bis(diolato) complex is stabi-

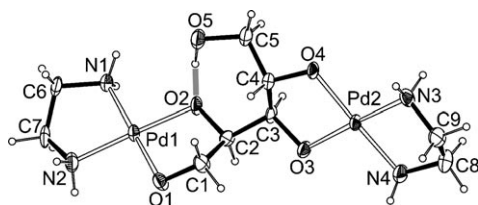


Figure 3. ORTEP plot (ellipsoids drawn at 60% probability) of the xylitol complex in **3**. Bond lengths (Å): Pd1–O2 2.004(3), Pd1–O1 2.006(3), Pd1–N1 2.021(4), Pd1–N2 2.030(3), Pd2–O3 1.983(3), Pd2–O4 1.993(3), Pd2–N4 2.046(4), Pd2–N3 2.049(4), C1–O1 1.429(5), C2–O2 1.434(5), C3–O3 1.435(5), C4–O4 1.430(5), C5–O5 1.431(5), C1–C2 1.520(6), C2–C3 1.537(6), C3–C4 1.518(7), C4–C5 1.526(6). Bond and torsion angles (°): O2–Pd1–O1 85.24(12), N1–Pd1–N2 84.08(15), C1–C2–C3 115.6(4), C4–C3–C2 117.0(4), O4–C4–C5 106.3(4), C3–C4–C5 112.8(4), O5–C5–C4 114.4(4); O1–C1–C2–O2 53.6(5), O3–C3–C4–O4 43.4(5). Donor–acceptor distance in the intramolecular hydrogen bond: O5...O2 2.506 Å.

lized by a δ hydrogen bond as short as that in **2**. Closer inspection of the environment of the individual alkoxy groups, however, reveals a difference between the binuclear pentitol structures, which may be the reason for the generally observed preference of binuclear complexes for *erythro*-linked bis(diolato) ligands. Whereas each of the alkoxy O atoms in the *erythro*-linked structures is an acceptor of two hydrogen

bonds, for steric reasons, the O3 atom in **3** accepts a single hydrogen bond only, with a water molecule as the donor. The second lone pair of electrons of this oxygen atom is clearly too close to the carbon backbone to bind another water molecule.

At an equimolar Pd/pentitol ratio, both arabitol as well as xylitol form the expected chelate ring according to the *threo* rule derived above (Table 4). Thus, [Pd(en)(D-Arab2,3H₂)] was the only monometalated species in 1:1 solutions for the former, the minor species being the stable dimetalated complex together with a molar equivalent of free arabitol. As the dimetalated complex is less predominant with xylitol, another monometalated species besides the main [Pd(en)(Xylt2,3H₂)] species was observable, namely, the terminally chelated [Pd(en)(Xylt1,2H₂)].

Owing to the lack of favorable *threo* chelation, ribitol is a particularly useful tool for investigating the rules derived above. Monometalation is reliably predictable: the [Pd(en)(Ribt1,2H₂)] species is expected to dominate over [Pd(en)(Ribt2,3H₂)] and, in fact, it does (Table 4). The dimetalated case is less unambiguous. The [Pd₂(en)₂(Ribt1,2;3,4H₄)] species showed the favorable *erythro*-linked bischelate, which is stabilized by a δ hydrogen bond between the donor hydroxy group at C5 and the O2 alkoxido ligand; this bond is missing in the [Pd₂(en)₂(Ribt1,2;4,5H₄)] species, but one of the Pd atoms does not reside in an *erythro* chelate. The ¹³C NMR spectra (Table 4) showed that the hydrogen-bonded complex is the more stable one; its bis(terminal) competitor is thus only a minor species.

D-Mannitol and Dulcitol: Hydrogen Bonding versus Metal Coordination

Hexitols are composed of three adjacent diol groups; hence, a maximum of three Pd(en) fragments may be expected to be bonded at high metal/polyol ratios. To investigate the competition between metalation and intramolecular hydrogen bonding, the two common symmetrical hexitols D-mannitol (D-Mann) and dulcitol (Dulc) were investigated.

By using a Pd/hexitol molar ratio of 1:1, the *threo* rule derived above was confirmed (Table 5). In fact, the *threo*-configured [Pd(en)(Dulc2,3H₂)] racemate was the only complex of 1:1 Pd/hexitol stoichiometry. Neither terminal (Dulc1,2H₂) nor *erythro* (Dulc3,4H₂) chelation were detected by ¹³C NMR spectroscopy, thus leaving, as is usual at the 1:1 ratio, only two additional species in the solution equilibrium: a dimetalated DulcH₄ species and the equivalent amount of free dulcitol. To examine the rules of monometalation, mannitol is a particularly suitable probe. The favored *threo* diol occurs only once in mannitol, but there are two terminal and *erythro*-configured diol groups. Accordingly, at the 1:1 Pd/Mann ratio, equal amounts of [Pd(en)(D-Mann1,2H₂)] and [Pd(en)(D-Mann3,4H₂)] were detected; *erythro* coordination did not appear competitive. Only weak signals were assigned to [Pd(en)(D-Mann2,3H₂)]. However, owing to accidental signal overlap and ambiguities regarding the correct assignment of signals to the individual carbon

Table 5. ^{13}C NMR chemical shifts (ppm) of the observed solution species in hexitol solutions of different Pd-en/hexitol molar ratios.^[a]

	C1	C2	C3	C4	C5	C6	3:1	2:1	1:1
Dulc	63.9	70.8	70.0				n.d.	n.d.	+
[Pd(en)(Dulc2,3H ₂)]	65.5	80.8	81.1	72.2	73.2	63.9	n.d.	–	++
($\Delta\delta$)	(1.6)	(10.0)	(11.1)	(2.2)	(2.4)	(0.0)			
[Pd ₂ (en) ₂ (Dulc2,3;4,5H ₄)]	64.8	83.3	84.9				++++	++++	+
($\Delta\delta$)	(0.9)	(12.5)	(14.9)						
D-Mann	63.9	71.5	69.9				n.d.	n.d.	+
[Pd(en)(D-Mann1,2H ₂)]	73.5 ^[b]	80.8	– ^[c]	– ^[c]	– ^[c]	63.9	n.d.	trace	+
($\Delta\delta$)	(9.6)	(9.3)				(0.0)			
[Pd(en)(D-Mann3,4H ₂)]	64.4	73.5	82.1				n.d.	–	+
($\Delta\delta$)	(0.5)	(2.0)	(12.2)						
[Pd ₂ (en) ₂ (D-Mann1,2;3,4H ₄)]	73.7	86.7	83.3	86.1	73.1	63.9	+++	+++	+
($\Delta\delta$)	(9.8)	(15.2)	(13.4)	(16.2)	(1.6)	(0.0)			
[Pd ₂ (en) ₂ (D-Mann1,2;5,6H ₄)]	73.5	80.8	71.0				–	–	trace
($\Delta\delta$)	(9.6)	(9.3)	(1.1)						
[Pd ₃ (en) ₃ (D-MannH ₆)]	75.1	83.3 ^[d]	81.6 ^[d]				+	–	n.d.
($\Delta\delta$)	(11.2)	(11.8)	(11.7)						

[a] Atoms numbered as in Scheme 1. The signals of the en ligand are omitted. $\Delta\delta$ values that indicate a CIS due to 1,2-diolate coordination are in bold. Chemical shifts are relative to D₂O/MeOH except for [Pd(en)(D-Mann1,2H₂)], [Pd₂(en)₂(D-Mann1,2;5,6H₄)], and [Pd₃(en)₃(D-MannH₆)], whose spectra were recorded in H₂O; to scale the measurements, 1.3 ppm has been added to the values for these species. As a rough assessment of the molar concentrations of the individual species, “+”=about 1/4 of the total hexitol concentration, “–”=about 10% or less, “trace”=NMR-detectable species, “n.d.”=not detected. [b] Coincidental with [Pd(en)(D-Mann3,4H₂)]-C2. [c] Assignment ambiguous, δ =71.8, 71.6, 70.8 ppm. [d] Signals may be interchanged.

atoms, this species is not included in Table 5. Therefore, the data for the tetritol species (Table 2) match the ligand properties of mannitol in terms of the particularly restricted ability of the *erythro*-configured diol moiety to act as a chelator.

At a higher Pd/hexitol ratio, the dimetalated species became the main solution species for both hexitols. In a reflection of the weakness of *erythro* chelation and the strength of the *erythro* link between two adjacent diol chelators, no symmetrical [Pd₂(en)₂(D-Mann2,3;4,5H₄)] species was detected in the spectra despite the fact that two intramolecular hydrogen bonds could be established to stabilize this hypothetical species. Instead, the main solution species was [Pd₂(en)₂(D-Mann1,2;3,4H₄)], which comprises pairwise terminal/*threo* chelation with an *erythro* link in between. The structure of the complex molecules in yellow crystals of [Pd₂(en)₂(D-Mann1,2;3,4H₄)]·6H₂O (**4**; Table 3) confirms the NMR spectroscopic result and highlights another structural feature: the δ hydrogen bond, which is clearly the most-stable type of intramolecular hydrogen bond in a polyolato ligand (Figure 4). As this δ bond is established in favor of an ϵ bond, the C6 terminus of the hexitol is left hanging without a particular function for the structure of the complex. Accordingly, another dimetalated species, [Pd₂(en)₂(D-Mann1,2;5,6H₄)], was detected as a minor component (Table 5).

In the case of dulcitol, all the optimum conditions for dimetalation coincide: each individual palladium atom is incorporated into a *threo* chelate, the two Pd binding sites are *erythro*-linked, and the terminal hydroxy groups can act as donors in δ hydrogen bonds. When the palladium content of the solution exceeded the Pd/Dulc ratio of 2:1, the result was a simple three-signal ^{13}C NMR spectrum of the expected C₁-symmetrical [Pd₂(en)₂(Dulc2,3;4,5H₄)] species. Crystallization from 2:1 solutions was successful. Structural anal-

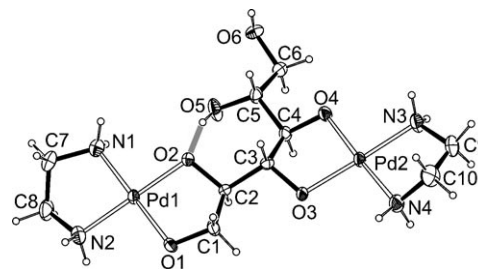


Figure 4. ORTEP plot (ellipsoids drawn at 60% probability) of the mannitol complex in **4**. Bond lengths (Å): Pd1–O2 1.999(2), Pd1–O1 2.000(2), Pd1–N1 2.034(2), Pd1–N2 2.047(2), Pd2–O4 1.977(2), Pd2–O3 2.012(2), Pd2–N3 2.042(2), Pd2–N4 2.047(2), C1–O1 1.435(3), C2–O2 1.441(3), C3–O3 1.436(3), C4–O4 1.418(3), C5–O5 1.423(3), C6–O6 1.426(3), C1–C2 1.500(4), C2–C3 1.539(3), C3–C4 1.541(3), C4–C5 1.536(3), C5–C6 1.513(3). Bond and torsion angles (°): O2–Pd1–O1 83.78(7), N1–Pd1–N2 83.77(9), C1–C2–C3 116.0(2), O3–C3–C4 106.4(2), C2–C3–C4 115.0(2), O4–C4–C5 106.5(2), C5–C4–C3 118.1(2), O5–C5–C6 105.6(2), O5–C5–C4 113.5(2), C2–O2–Pd1 105.80(15), O1–C1–C2–O2 51.9(2), O3–C3–C4–O4 –55.6(2). Donor–acceptor distance in the intramolecular hydrogen bond: O5···O2 2.533 Å.

ysis of [Pd₂(en)₂(Dulc2,3;4,5H₄)]·6H₂O (**5**) showed the dulcitolato ligand as the same rigid bis(diolato) ligand found in copper(II) and nickel(II) complexes in our previous work (Figure 5 and Table 6).^[8]

The conservative formation of the Pd₂(Dulc2,3;4,5H₄) pattern is underlined by experiments with the sterically more demanding Pd^{II}(MeNH₂)₂ metal fragment. The addition of dulcitol to a 0.3 M solution of [Pd^{II}(MeNH₂)₂(OH)₂] according to a Pd/polyol molar ratio of 3.5:1 yielded a yellow solution that contained the binuclear Pd₂(Dulc2,3;4,5H₄) core, as shown by the ^{13}C NMR spectra. The diffusion of acetone vapor at 4 °C resulted in the formation of yellow crystals over the course of three weeks. Struc-

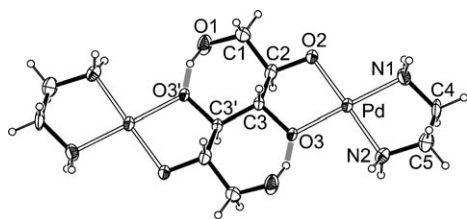


Figure 5. ORTEP plot (ellipsoids drawn at 70% probability) of the C_1 -symmetric dulcitolato(4 $-$) complex in **5**. Bond lengths (\AA): Pd–O3 1.999(3), Pd–O2 2.010(3), Pd–N2 2.043(4), Pd–N1 2.042(4), O1–C1 1.427(6), O2–C2 1.429(5), O3–C3 1.442(5), C1–C2 1.520(6), C2–C3 1.535(5), C3–C3' 1.515(8). Bond and torsion angles ($^\circ$): O3–Pd–O2 83.97(12), N2–Pd–N1 83.89(15), O1–C1–C2 113.1(4), C1–C2–C3 118.0(3), O3–C3–C2 105.3(3), C3'–C3–C2 117.2(4); O2–C2–C3–O3 56.2(4). Donor–acceptor distance in the two intramolecular hydrogen bonds: O1 \cdots O3' 2.526 \AA .

Table 6. Crystallographic data of the dulcitolato complexes **5**, **6**, and **8**.

	5	6	8
Net formula	$C_{10}H_{38}N_4O_{12}Pd_2$	$C_{16}H_{62}N_4O_{18}Pd_2$	$C_{30}H_{96}Cl_2N_8O_{22}Pd_4$
M_r [g mol^{-1}]	619.24	811.50	1417.71
Crystal size [mm]	$0.13 \times 0.05 \times 0.03$	$0.20 \times 0.10 \times 0.08$	$0.27 \times 0.11 \times 0.01$
T [K]	200(3)	200(3)	200(3)
Diffractionmeter	Stoe IPDS	Stoe IPDS	KappaCCD
Crystal system	triclinic	monoclinic	triclinic
Space group	$P\bar{1}$	$P2_1/c$	$P\bar{1}$
a [\AA]	7.422(1)	7.3422(5)	7.7660(2)
b [\AA]	9.278(2)	19.580(2)	13.0114(4)
c [\AA]	9.636(2)	12.5550(9)	14.0568(4)
α [$^\circ$]	117.71(1)	90	78.341(1)
β [$^\circ$]	91.58(2)	104.104(8)	76.285(2)
γ [$^\circ$]	104.73(2)	90	81.223(2)
V [\AA^3]	559.9(2)	1750.5(2)	1343.22(7)
Z	1	2	1
ρ_{calcd} [g cm^{-3}]	1.8366(7)	1.5397(2)	1.75265(9)
μ [mm^{-1}]	1.666	1.098	1.494
Absorption correction	none	numerical	numerical
Transmission factors	–	0.8397–0.9433	0.7924–0.9819
Reflections measured	5127	8905	13219
R_{int}	0.0497	0.0545	0.0513
Mean $\sigma(I)/I$	0.0653	0.0523	0.0504
θ range	2.42–28.04	2.08–23.00	2.39–23.00
Observed refls.	1908	1842	3211
x, y (weighting scheme)	0.0410, 0	0.0394, 0	0.0657, 0.9463
Reflections in refinement	2404	2400	3735
Parameters	150	221	348
Restraints	9	0	25
$R(F_{\text{obs}})$	0.0320	0.0315	0.0377
$R_w(F^2)$	0.0776	0.0690	0.1143
S	0.984	0.923	1.140
Shift/error $_{\text{max}}$	0.001	0.001	0.001
Max. electron density [e \AA^{-3}]	0.929	0.768	0.988
Min. electron density [e \AA^{-3}]	–1.419	–0.468	–1.124

tural analysis of monoclinic crystals of $\{[\text{Pd}(\text{MeNH}_2)(\text{Me}_2\text{C}=\text{NMe})_2(\text{Dulc}2,3,4,5\text{H}_4)] \cdot 6\text{H}_2\text{O}$ (**6**; Table 6) revealed partial

transformation of one of the two methylamine ligands. Condensation with the precipitating agent acetone led to the formation of the isopropylidene methylimine ligand (Figure 6). The S-shaped dulcitolato ligand gave almost identical structural data for **5** and **6** in terms of torsion angles and hydrogen-bond distances.

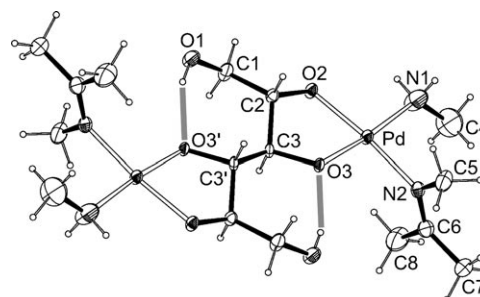


Figure 6. ORTEP plot (ellipsoids drawn at 40% probability) of the C_s -symmetric dulcitolato(4 $-$) complex in **6**. Bond lengths (\AA): Pd–O2 1.997(3), Pd–O3 1.986(2), Pd–N1 2.044(4), Pd–N2 2.022(4). Bond and torsion angles ($^\circ$): O2–Pd–O3 84.3(1), N1–Pd–N2 92.6(2), O3–C3–C2 106.0(3), C2–C3–C3' 116.2(4), C1–C2–C3 117.3(4); O3–C3–C2–O2: 53.9(4). Donor–acceptor distance in the two intramolecular hydrogen bonds: O1 \cdots O3' 2.537(5).

With the various contributions to the overall stability of a metal complex of a particular hexitol configuration in mind, complete metalation at high Pd/hexitol ratios appears possible for mannitol but a challenge in the case of dulcitol. In fact, the three signals of the $[\text{Pd}_3(\text{en})_3(\text{D-Mann}1,2,3,4;5,6\text{H}_6)]$ species were detected in such solutions of mannitol (Table 5). In the case of dulcitol, however, not even a trace of trimetalated species was observed.

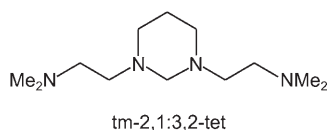
Shift Patterns in ^{13}C NMR Spectra

Although the ^{13}C NMR signal assignments made in Tables 2, 4, and 5 were derived from correlated spectra, the resulting shifts, particularly the CIS values, support the assignments made by a consistent pattern of chemical-shift values. As shown by the data for the dimetalated species, chelation of the palladium center resulted in a 9–11-ppm CIS of the respective carbon signal. This range was shifted to 11–12 ppm if a carbon atom of one chelate ring is adjacent to a carbon atom of another. The only factor that remains to be considered at this point is δ hydrogen bonding. With the exception of xylitol, all the δ -bond-supported bischelates are *erythro*-linked. In these molecules, the downfield shift of the chelate carbon signals is in the 12–16-ppm range. The xylitol case is different. An unusual 15.0–7.8-ppm CIS pattern was observed for the 3,4 chelate, that is, the CIS of the C4 signal is unexpectedly low. However, this result seems to be typical and indicative of this stereochemistry. Preliminary data on D-iditol (D-Idit), the only hexitol with an all-*threo* configuration, showed almost identical shifts. At the 3:1 ratio, the main solution species exhibited three signals. The clearly C_2 -

symmetrical D-iditolato ligand constitutes the species $[\text{Pd}_2(\text{en})_2(\text{D-Idit}2,3;4,5\text{H}_{-4})]$, and the respective CIS pattern was 15.3–7.9 ppm, close to that of xylitol.

Forcing Full Metalation: Binucleating Nitrogen Ligands

The competition between metal bonding to suitable coordination sites and intramolecular hydrogen bonding towards the strong alkoxy acceptors appears to be the determining factor for the structures of the compounds described above. At the outset, an open-chain compound such as dulcitol might have been supposed to be flexible. This work, however, demonstrates that the coincidence of suitable factors for dimetalation is capable of completely restricting the accessible conformations of a polyolato ligand to a single one. Further deprotonation and metalation of the Dulc2,3;4,5H₋₄ ligand thus emerges as a challenge for the design of metal-spectator-ligand fragments that are able to compete with strong hydrogen bonding. Attempts to construct metal fragments that can cleave the intramolecular hydrogen bond of the DulcH₋₄ entity were successful for the 1,3-bis(2'-dimethylaminoethyl)hexahydropyrimidine (tm-2,1:3,2-tet) ligand (Scheme 3).



Scheme 3. The 1,3-bis(2'-dimethylaminoethyl)hexahydropyrimidine ligand in **7** and **8**.

The dinuclear metal educt was prepared by reaction of the tetradentate nitrogen ligand with bis(benzonitrile)dichloropalladium(II) and subsequent replacement of chloro by hydroxo ligands. Yellow crystals of $[\text{Pd}_2(\text{tm-2,1:3,2-tet})(\text{OH})_3]\text{Cl}\cdot 8\text{H}_2\text{O}$ (**7a**) were isolated from these solutions upon incomplete chloride/hydroxide exchange.^[9] On the basis of this structure determination, the alkaline aqueous solution of the palladium reagent itself was determined to be that of $[\text{Pd}_2(\text{tm-2,1:3,2-tet})(\text{OH})_3]\text{OH}$ (**7b**).

After the reaction of 0.2 M of **7b** with dulcitol, a C_i-symmetric species was formed, as indicated by three signals in the dulcitol part of the ¹³C NMR spectrum ($\delta=90.4$, 78.4, 73.7 ppm). The CIS pattern is consistent with full metalation of the polyol: the atypically large CIS of 19.6 ppm indicates a bridging position of the C2/5 atoms, whereas the other carbon atoms are clearly connected to a single Pd atom (CIS values: 8.4 ppm for C3/4, 9.8 ppm for C1/6). The addition of chloride yielded crystals of $[\text{Pd}_4(\text{tm-2,1/3,2-tet})_2(\text{DulcH}_{-6})]\text{Cl}_2\cdot 16\text{H}_2\text{O}$ (**8**). Structural analysis confirmed the spectroscopic result (Figure 7 and Table 6). Due to the bonding of four palladium centers, full deprotonation was forced, and there are no longer intramolecular hydrogen bonds in the complex dication. A comparison of the bond angles along the dulcitol-carbon chains of **5**, **6**, and **8** shows

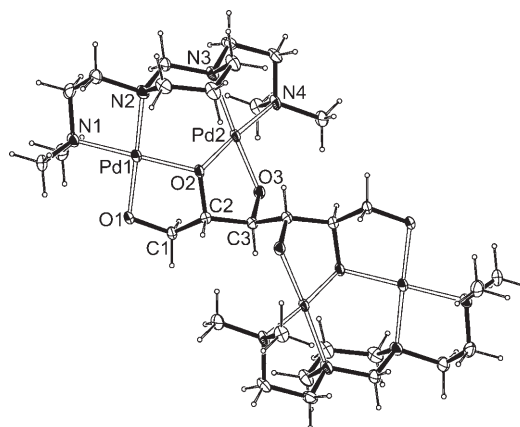


Figure 7. ORTEP plot (ellipsoids drawn at 30% probability) of the C_i-symmetric dulcitolato(6-) complex in **8**. Bond lengths (Å): Pd1–O1 1.989(3), Pd1–O2 2.004(3), Pd1–N1 2.047(4), Pd1–N2 2.082(4), Pd2–O3 1.968(3), Pd2–O2 2.011(3), Pd2–N4 2.050(4), Pd2–N3 2.105(4); Pd1...Pd2 3.2373(5). Bond and torsion angles (°): O1–Pd1–O2 85.6(1), N1–Pd1–N2 87.1(2), O2–Pd2–O3 84.7(1), N4–Pd2–N3 86.2(2), Pd1–O2–Pd2 107.48(2); O1–C1–C2–O2 –47.7(5), O2–C2–C3–O3 –49.7(5).

that the release of the intramolecular hydrogen bonds lifts the angle strain that is typical for the Dulc2,3;4,5H₋₄ ligand (Figures 5–7; note the 3° criterion described in the Experimental Section). Owing to the coordination of four instead of two metal centers, hydrogen bonding is generally of less importance in crystals of **8**. The bridging O2 atom does not accept any hydrogen bonds and uses its bonding capability exclusively for metal binding. O3 acts as the acceptor of a single hydrogen bond with a water molecule as the donor. Only the terminal O1 atom accepts two hydrogen bonds from two different water molecules.

Conclusions

Sugar alcohols, although open-chain carbohydrate derivatives, are by no means the flexible ligands they are expected to be. Most surprisingly, the ability of these polyfunctional molecules to offer a variety of metal-binding sites is not governed by the chain length. Instead, a couple of stereochemical rules determine the ligand properties. Thus, the highest stability is found if 1) the individual chelate ring is formed by a *threo*-configured diol group, 2) two adjacent chelating diol groups are *erythro*-linked, and 3) a δ hydrogen bond, that is, a hydrogen bond whose donor hydroxy and acceptor alkoxido parts are separated by a C₄ chain, can be established. If a specific metalation pattern matches all these conditions—an example is given with dimetalated dulcitol—the polyolato ligand is invariably found in this bonding situation. If not, a variety of species of comparable stability is then present in solution.

Conversely, it is a challenge to force full deprotonation and metalation of a ligand such as dulcitolato(4-). Because a powerful competitor to strong hydrogen bonding is needed, a simple reagent such as Pd-en can no longer be

used for the purpose of full metalation. Instead, tailor-made complexing agents that are adapted to the particular alkoxydo pattern to be supported are needed.

Experimental Section

Syntheses

General procedure for the preparation of Pd(en) complexes: Aqueous solutions of Pd-en (0.2–0.4 M) were prepared according to the method in the literature.^[3b] The respective polyol was added to the amounts given above. The solutions were stirred for 2 h at 0 °C. NMR spectra of these solutions were recorded. For crystallization, acetone vapor from acetone/water mixtures was allowed to diffuse into the solutions at room temperature. To obtain crystals of good quality, crystallization was interrupted at a typical yield of 30%. Complex **1** formed from 0.4 M Pd-en without the addition of a precipitant over the course of 2 days.

Bis(benzonitrile)dichloropalladium(II): The procedure of reference [10] was slightly modified: palladium(II) chloride (4.10 g, 23.0 mmol) and benzonitrile (100 mL) were heated to 120 °C for 30 min under stirring, after which the mixture was filtered. The filtrate was cooled to 30 °C, and pentane (600 mL) was added. After the mixture was cooled to 4 °C for 2 h, the yellow precipitate was filtered off, washed with pentane, and dried in vacuo to give bis(benzonitrile)dichloropalladium(II) (8.4 g, 22 mmol, 96 %).

tm-2,1:3,2-tet: *N,N*-Dimethyl-1,2-diaminoethane (100 mL, 80.7 g, 0.915 mol) was heated to 40 °C. 1,3-Dibromopropane (28.0 mL, 55.4 g, 0.274 mol) was added with vigorous stirring over the course of 2 h. After the mixture was heated to 80 °C for 1 h, the resulting suspension was dissolved in NaOH (500 mL, 0.4 M). The solution was extracted with trichloromethane (3 × 200 mL). The combined organic layers were dried with sodium sulfate, and the solvent was removed. Fractional vacuum distillation (90 °C, 4.7×10^{-2} mbar) yielded 1,3-bis[2'-(dimethylamino)ethylamino]propane as a colorless oil (10.6 g, 49 mmol, 18% relative to dibromopropane). ¹³C{¹H} NMR (CDCl₃): δ = 30.3, 45.3, 47.2, 48.2, 58.9 ppm. The tetraamine was then dissolved in water (15 mL). Formaldehyde (4.5 mL, 53 mmol) was slowly added to the cooled solution with stirring, which was continued for 30 min. The solution was extracted with trichloromethane (3 × 100 mL). The combined organic layers were dried with sodium sulfate, and the solvent was removed. Fractional vacuum distillation (74 °C, 10^{-3} mbar) yielded 1,3-bis[2'-(dimethylamino)ethyl]hexahydropyrimidine (tm-2,1:3,2-tet) as a colorless oil (9.6 g, 42 mmol, 86% relative to the tetraamine educt). ¹³C{¹H} NMR (CDCl₃): δ = 23.5, 46.2, 53.1, 53.5, 57.8, 77.0 ppm.

7b: Bis(benzonitrile)dichloropalladium(II) (5.0 g, 13.2 mmol) was dissolved in dichloromethane (250 mL) and acetonitrile (250 mL). tm-2,1:3,2-tet (1.5 g, 6.6 mmol), dissolved in dichloromethane (100 mL), was added over the course of 10 min. After the mixture was stirred for 2 h, the yellow precipitate was filtered off and dried in vacuo (3.5 g, 6.0 mmol, 91%). Silver(I) oxide (2.9 g, 12.5 mmol) and water (30 mL) were then added. The suspension was stirred for 15 min in the dark and filtered. The yellow filtrate, an alkaline aqueous solution of **7b** (0.2 M), was stable for months when stored under nitrogen at 4 °C in the dark. ¹³C{¹H} NMR (H₂O): δ = 20.1 (1 C, CH₂CH₂CH₂), 49.0 (2 C, CH₃), 50.9 (2 C, CH₃), 57.3 (2 C), 60.0 (2 C), 60.4 (2 C), 80.7 (1 C, NCH₂N).

8: Dulcitol (73 mg, 0.40 mmol) and lithium chloride (25 mg, 0.59 mmol) were stirred in an aqueous solution of **7b** (3.0 mL, 0.6 mmol, 0.2 M) at room temperature for 2 days. Acetone vapor was allowed to diffuse from an acetone/water mixture (5:1) at room temperature until yellow platelets of **8** formed.

Crystal-Structure Analysis

Crystals suitable for X-ray crystallography were selected by means of a polarization microscope, mounted on the tip of a glass fiber, and subjected to XRD on either a Nonius Kappa CCD or a Stoe IPDS diffractometer, both with graphite-monochromated MoK α radiation (λ = 0.71073 Å). The structures were solved by direct methods (SIR 97, SHELXS) and refined by full-matrix least-squares calculations on *F*² (SHELXL-97). Anisotropic displacement parameters were refined for all non-hydrogen atoms. Crystallographic data are shown in Tables 3 and 6. The number of restraints given refers to DFIX restraints. Bond angles in the polyolato ligand are given in the tables if they deviate more than 3° from the tetrahedral angle. CCDC-617676 (**1**), -617677 (**2**), -617678 (**3**), -617679 (**4**), -618044 (**5**), -617680 (**6**), and -617681 (**8**) contain the supplementary crystallographic data for this paper. These data can be obtained free of charge from The Cambridge Crystallographic Data Centre at www.ccdc.cam.ac.uk/data_request.cif.

NMR Spectroscopy

¹³C{¹H} NMR spectra were recorded by using 1 mL of filtered reaction mixture in a 5-mm tube. Equipment used: Jeol EX-400, GSX 270, 400e spectrometers. Signal assignment was based on distortionless enhancement by polarization transfer (DEPT) and two-dimensional techniques. All δ values given relative to δ = 49.5 ppm for methanol in D₂O as internal reference.

- [1] In this work, the deprotonated hydroxy groups resemble the metal-binding O atoms. Hence, the ligand formula α -D-Glcp1,2,3,4H₄- κ^2 O¹,O²: κ^2 O³,O⁴ is abbreviated as α -D-Glcp1,2;3,4H₄ throughout (the semicolon separates the chelating sites).
- [2] a) P. Klüfers, T. Kunte, *Angew. Chem.* **2001**, *113*, 4356–4358; *Angew. Chem. Int. Ed.* **2001**, *40*, 4210–4212; b) P. Klüfers, T. Kunte, *Chem. Eur. J.* **2003**, *9*, 2013–2018.
- [3] a) J. Burger, G. Kettenbach, P. Klüfers, *Macromol. Symp.* **1997**, *120*, 291–301; b) R. Ahlrichs, M. Ballauff, K. Eichkorn, O. Hanemann, G. Kettenbach, P. Klüfers, *Chem. Eur. J.* **1998**, *4*, 835–844.
- [4] P. Klüfers, T. Kunte, unpublished results.
- [5] M. A. Andrews, E. J. Voss, G. L. Gould, W. T. Klooster, T. F. Koetzle, *J. Am. Chem. Soc.* **1994**, *116*, 5730–5740.
- [6] X. Kästle, P. Klüfers, T. Kunte, *Z. Anorg. Allg. Chem.* **2001**, *627*, 2042–2044.
- [7] P. Klüfers, E. Önem-Siakou, unpublished results.
- [8] a) P. Klüfers, J. Schuhmacher, *Angew. Chem.* **1994**, *106*, 1839–1841; *Angew. Chem. Int. Ed. Engl.* **1994**, *33*, 1742–1744; b) S. Herdin, P. Klüfers, T. Kunte, H. Piotrowski, *Z. Anorg. Allg. Chem.* **2004**, *630*, 701–705.
- [9] Y. Arendt, P. Klüfers, unpublished results.
- [10] G. Brauer, *Handbuch der präparativen anorganischen Chemie*, Vol. 3, Ferdinand Enke, Stuttgart, **1981**.

Received: March 21, 2007
Published online: June 19, 2007